LETTER

Fusion product losses due to fishbone instabilities in deuterium JET plasmas

IOP Publishing | International Atomic Energy Agency Nuclear Fusion

Nucl. Fusion **58** (2018) 014003 (6pp) https://doi.org/10.1088/1741-4326/aa9340

Letter

Fusion product losses due to fishbone instabilities in deuterium JET plasmas

V.G. Kiptily[1], M. Fitzgerald[1], V. Goloborodko[2], S.E. Sharapov[1], C.D. Challis[1], D. Frigione[3], J. Graves[4], M.J. Mantsinen[5,6], P. Beaumont[1], M. Garcia-Munoz[7], C. Perez von Thun[8,9], J.F.R. Rodriguez[7], D. Darrow[10,a], D. Keeling[1], D. King[1], K.G. McClements[1], E.R. Solano[11], S. Schmuck[1], G. Sips[12], G. Szepesi[1] and JET Contributors[b]

[1] Culham Centre for Fusion Energy, UKAEA, Culham Science Centre, Abingdon, OX14 3DB, United Kingdom
[2] OEAW, Institute for Theoretical Physics, University of Innsbruck, Innsbruck, Austria
[3] Unità Tecnica Fusione, ENEA C. R. Frascati, via E. Fermi 45, 00044 Frascati (Roma), Italy
[4] Ecole Polytechnique Fédérale de Lausanne, Swiss Plasma Center, CH-1015 Lausanne, Switzerland
[5] Barcelona Supercomputing Center, Barcelona, Spain
[6] ICREA, Pg. Liuis Companys 23, 08010 Barcelona, Spain
[7] Faculty of Physics, FAMN Department, University of Seville, 41012 Seville, Spain
[8] EUROfusion Programme Management Unit, Culham Science Centre, Culham, OX14 3DB, United Kingdom
[9] Forschungszentrum Jülich GmbH, Institut für Energie-und Klimaforschung—Plasmaphysik, 52425 Jülich, Germany
[10] Princeton Plasma Physics Laboratory, Princeton, NJ 08543, United States of America
[11] Laboratorio Nacional de Fusión, CIEMAT, Madrid, Spain
[12] European Commission, B-1049 Brussels, Belgium

E-mail: vasili.kiptily@ukaea.uk

Received 20 July 2017, revised 9 October 2017
Accepted for publication 13 October 2017
Published 8 November 2017

Abstract

During development of a high-performance hybrid scenario for future deuterium–tritium experiments on the Joint European Torus, an increased level of fast ion losses in the MeV energy range was observed during the instability of high-frequency $n = 1$ fishbones. The fishbones are excited during deuterium neutral beam injection combined with ion cyclotron heating. The frequency range of the fishbones, 10–25 kHz, indicates that they are driven by a resonant interaction with the NBI-produced deuterium beam ions in the energy range $\leqslant$120 keV. The fast particle losses in a much higher energy range are measured with a fast ion loss detector, and the data show an expulsion of deuterium plasma fusion products, 1 MeV tritons and 3 MeV protons, during the fishbone bursts. An MHD mode analysis with the MISHKA code combined with the nonlinear wave-particle interaction code HAGIS shows that the loss of toroidal symmetry caused by the $n = 1$ fishbones affects strongly the confinement of non-resonant high energy fusion-born tritons and protons by perturbing their orbits and expelling them. This modelling is in a good agreement with the experimental data.

Keywords: tokamak, fusion products, MHD

(Some figures may appear in colour only in the online journal)

[a] Now deceased.
[b] See the author list of [20].

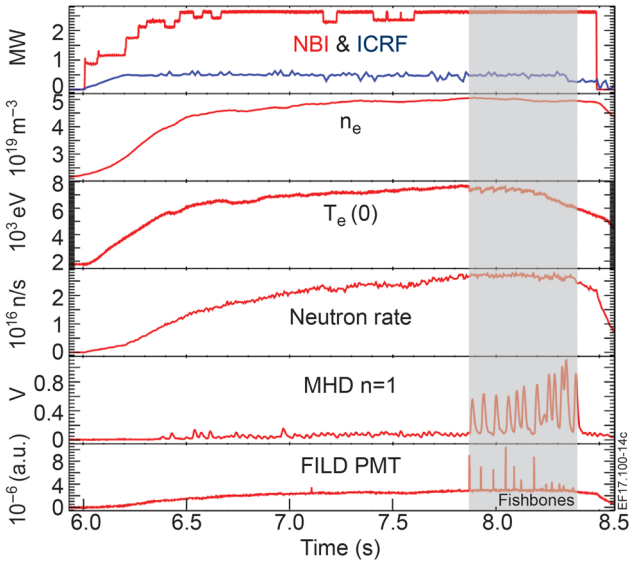

Figure 1. Waveforms of the deuterium plasma discharge #92394 at $B_T(0) = 2.8$ T, $I_P = 2.2$ MA with 26 MW deuterium NBI and 5 MW hydrogen 1st harmonic ICRH at $f_{ICRH} = 42.5$ MHz. Losses recorded with FILD PMTs correlate with fishbones excited during period indicated by shaded area.

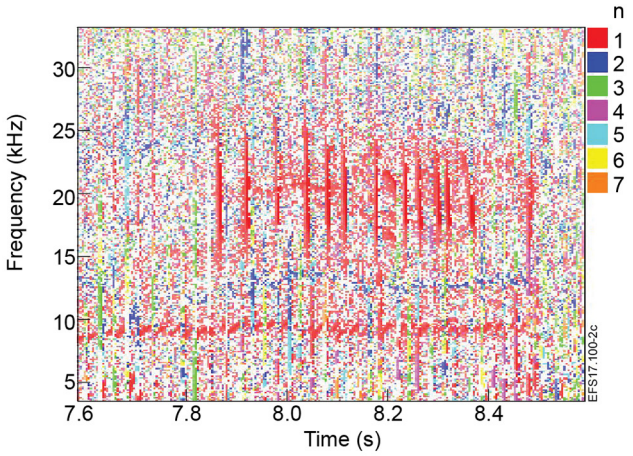

Figure 2. Fishbones with toroidal mode number $n = 1$ detected with Mirnov coils in the JET discharge #92394.

Fusion reactions as well as additional heating of fusion-grade tokamak plasmas generate large numbers of fast ions in the plasma core that can interact with the magneto-hydro-dynamic (MHD) perturbations of the plasma discharge. The MHD instabilities can eject fusion products (FP), in particular alpha-particles, which are the principal source of plasma heating in burning deuterium–tritium (D–T) plasmas. The interactions between MHD perturbations and alpha-particles could be resonant if the alpha-particles are in resonance with high-frequency waves, e.g. Toroidal Alfvén Eigenmodes (TAE) or non-resonant, when MHD perturbations are driven by thermal plasma or fast particles other than the alpha-particles. Both resonant and non-resonant interactions between alpha-particles and MHD perturbations could lead to the particle redistribution and losses [1] thus affecting the fusion plasma $Q = P_{out}/P_{in}$ and the first wall.

The development of high fusion performance scenarios, both 'baseline' sawtoothing H-mode with safety factor at the magnetic axis $q_0 \leqslant 1$ and the so-called 'hybrid' with $q_0 \geqslant 1$, for the forthcoming high-power D–T experiments was a main priority of recent deuterium and hydrogen experimental campaigns on the Joint European Torus (JET) with ITER-like wall. In the hybrid scenario with a low magnetic shear in the plasma centre [2], the sawtooth oscillations are almost always avoided but a strong beam ion pressure drives fishbones (FB) with toroidal mode number $n = 1$, an instability with bursting amplitude and sweeping frequency in the range ≈10–25 kHz.

The fishbones occur in plasmas with high-$\beta_{poloidal}$ (ratio of plasma pressure to poloidal magnetic field pressure) and they are destabilized by energetic ions produced from perpendicular and tangential neutral beam injection [3, 4], which in the case of JET experiments had primary energies 90 keV and 110 keV. As it has been shown [5, 6], trapped and circulating beam ions can resonate with fishbone perturbation, the core-localised $m = 1/n = 1$ mode. In JET and other tokamaks with fusion reactivity dominated by beam-plasma fusion reactions, neutron rate drops up to 10% were observed and linked to the resonant interaction between the beam ions and fishbones [7, 8].

In addition to the well-understood resonant interaction described in [5–8], the presence of fishbones also affects significantly the confinement of non-resonant ions in the MeV energy range. These ions are p, t and ^{3}He produced in the deuterium plasma due to the following fusion reactions:

$D + D = p\,(3\,\text{MeV}) + t\,(1\,\text{MeV})$ $D + D = n\,(2.5\,\text{MeV}) + {}^3\text{He}\,(0.82\,\text{MeV})$. During the fishbone periods, a 'burn-up' of tritons and ^{3}He was reduced. The reduction of the burn-up was measured via 14.1 MeV neutrons produced in the $D(t, n)^4$He fusion reaction and 14.7 MeV protons generated in another fusion reaction $D(^3\text{He}, p)^4$He. The anomalously low burn-up rate during fishbones has been explained by prompt and non-prompt losses of MeV-particles [9–11]. However, a part of the non-prompt losses, e.g. slow tritons, could be due to the resonant mechanism of interaction with fishbones (the cross-section has a maximum at $E_t \approx 160$ keV), as it was observed with the resonant beam particles. An early study of fusion product losses via the ^{3}He burn-up measurements (the cross-section has a maximum at $E_{^3\text{He}} \approx 650$ keV) was made on tokamak PDX [10]. In spite of the small size of the machine (a low rate of the $D(^3\text{He}, p)^4$He reaction), it was possible to identify the non-resonant character of the ^{3}He losses, and draw a conclusion on the possible applicability of the loss mechanism to ignition experiments.

A non-resonant loss mechanism due to high amplitude fishbones causing a distortion of the toroidal symmetry with the $m = 1/n = 1$ perturbation, was predicted for non-resonant alphas in burning plasmas in [12]. Experimentally, such non-resonant losses of fast ions in the MeV energy range caused by the fishbones driven by the beam deuterons with energy 80–100 keV were observed in JET discharges with ion cyclotron range of frequencies (ICRF) heating [13]. The high energy particles ejected from the plasma during the FB oscillations were identified as H-ions accelerated during ICRH. The losses were enhanced by about a factor of ≈10–20 with respect to

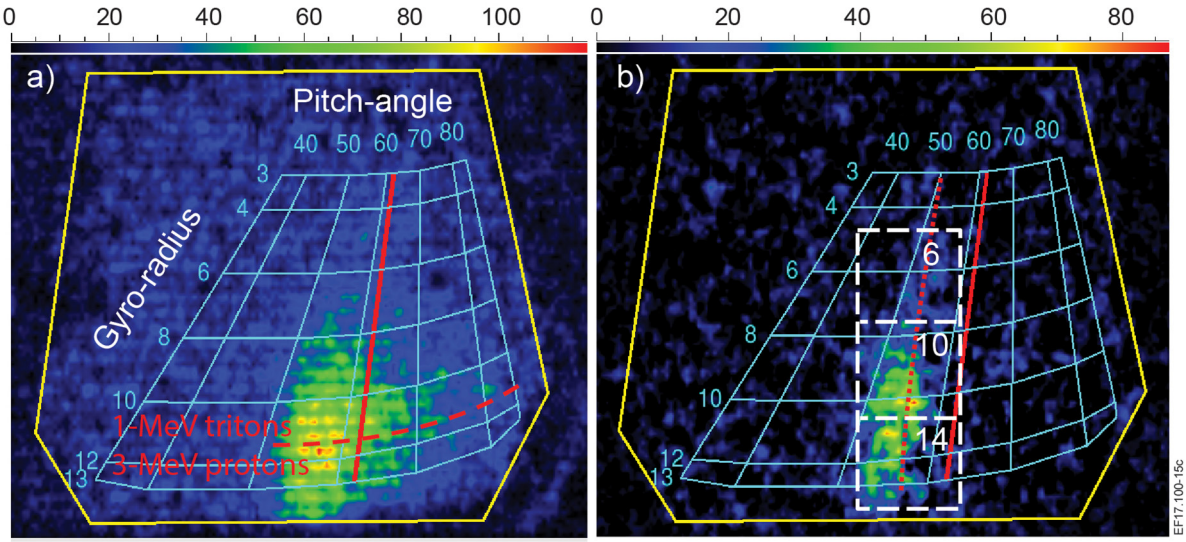

Figure 3. Footprints of losses in the discharge #92394 recorded with CCD camera: (*a*) in the period 7.843 s–7.860 s before a fishbone; red solid line—a position of the IC resonance on the gyro-radius versus pitch-angle grid; red dash line—gyro-radius related to fusion products: 1 MeV tritons and 3 MeV protons; (*b*) during the fishbone period 7.860 s–7.877 s obtained by subtraction of the signal in previous time bin (see (*a*)); the red dot line related to a separatrix between trapped and circulating orbits in the phase space; the white areas show fields of view by PMT #6, #10 and #14.

the MHD-quiescent levels, and the magnitude of the losses was found to increase quadratically with the FB amplitude.

In this Letter, we report on directly measured non-resonant losses of fusion protons and tritons in high performance experiments with hybrid plasmas. The fishbones were observed to trigger sawtooth-like reconnection events and neoclassical tearing modes (NTM), the latter substantially reducing the plasma performance.

JET is equipped well for the studies of confined and escaped fast ions [14]. The lost ion measurements are carried out with a scintillator probe [15], which is called 'fast ion loss detector', or FILD. FILD is located about 28 cm below the mid-plane of the torus, just outside the plasma and provides information on the lost ion pitch angle, $\theta = \cos^{-1}\left(v_{\|}/v\right)$, with 5% resolution in the range 35°–85° and gyro-radius between 3 cm and 14 cm with 15% resolution (for 12 cm gyro-radius ~2 cm). The light emitted by the scintillator (decay time ~0.5 μs) during an ion collision, is transferred through a coherent fibre bundle to a charge-coupled device (CCD) camera and a photomultiplier tube (PMT) 4 × 4 array. The 128 × 256 pixel CCD camera can provide 20 kHz snapshots of light emission on the pitch-angle—gyro-radius grid calculated with the EfipDesign code [16]. The FILD has recently been upgraded, so the fast PMT signals are digitised by 2 MHz thus allowing a loss spectrogram to be made with the MHz bandwidth. Such loss spectrograms could be then compared to magnetic spectrograms showing the MHD perturbations.

In the hybrid scenario experiments, with plasma currents in the range $I_P = 2.0$–2.4 MA at central toroidal field $B_T(0) = 2.8$ T, deuterium neutral beam injection (NBI) and H-minority heating of deuterium plasmas with ICRF at $f = \omega/(2\pi) \approx 42.5$ MHz of dipole phasing with hydrogen concentration $n_H/(n_H + n_D) \approx 1$–$3\%$ were used. Fishbones were observed in discharges with normalized poloidal beta $\beta_N > 1.9$, however not all of them led to the FP losses. A typical example of a discharge with fast ion losses during period of strong FB instabilities is shown in figure 1. The MHD instability in this discharge has been identified as $n = 1$ fishbones by means of a comparison of the signal phase in toroidally-separated Mirnov coils. The result of the mode analysis is presented on figure 2.

An example of losses measured with the FILD in discharge #92394 is shown in the gyro-radius (R_{gyr}) versus the pitch-angle grid in figure 3(*a*). This is a typical fusion product first orbit (FO) loss footprint recorded with CCD camera in the FB-free period 7.843 s–7.860 s just before a fishbone. It is clearly seen that the maxima of losses are localised along the gyro-radius (red dash line), corresponding to the FP birth energies, 1 MeV for tritons and 3 MeV for protons. Prompt ICRH losses, H-ions and D-NBI ions accelerated at $\omega = \omega_{cH} = 2\omega_{cD}$, would be expected to occur along the red solid line, corresponding to the IC resonance layer in the plasma, but such losses appear to be rather low. The image of losses recorded during the fishbone period 7.860 s–7.877 s is presented in figure 3(*b*). This image was obtained by a subtraction of the signal recorded during the previous no fishbone time bin shown in figure 3(*a*). It is important to note that the loss ion image obtained by the subtraction of the signal recorded after the FB period, 7.877 s–7.893 s, is indistinguishable from the one shown in figure 3(*b*). One can see that the losses related to the FB instability are localised along the red dot line, which is a separatrix between trapped and circulating orbits in the phase space. This indicates that the fishbone perturbation causes losses by pushing core-localised fusion products with confined passing orbits to a phase space area corresponding to the unconfined trapped orbits.

The FILD data analysis shows that in the FB period the fusion tritons and proton prompt losses are localised at the pitch-angle θ ~ 55° and the gyro-radius R_G ~ 11 cm that is related to a maximal signal. The gyro-radius distribution associated with the energy distribution has roughly the same

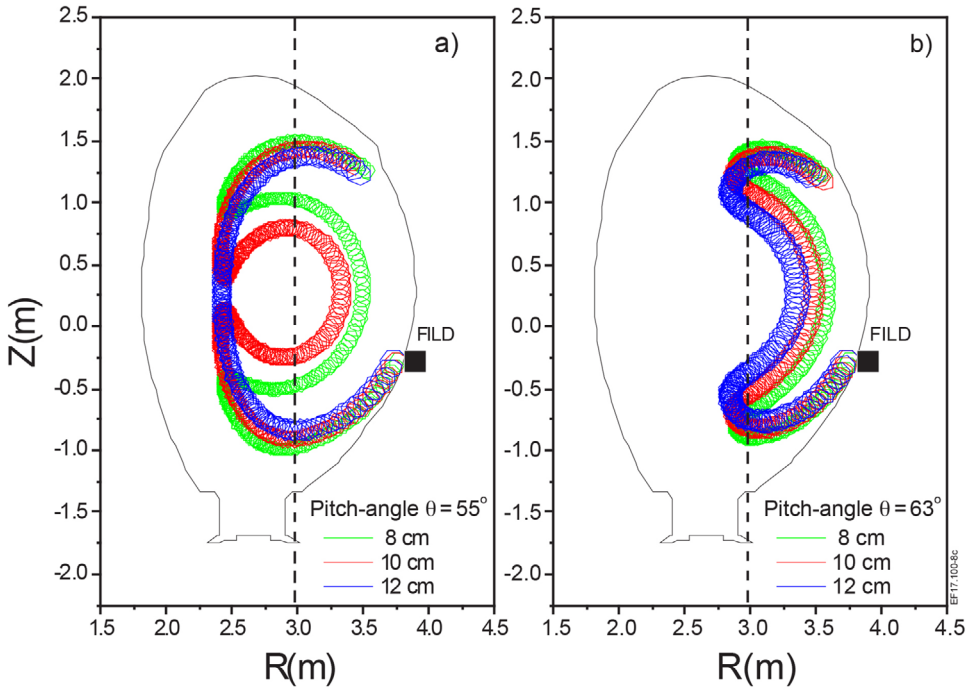

Figure 4. (*a*) orbits of tritons/protons with gyro-radii 8, 10 and 12 cm and pitch-angle 55° calculated back in time from the FILD scintillator plate; these parameters are related to the footprint presented in figure 3(*b*); black dash line—a position of the IC resonance $\omega = \omega_{cH}$; (*b*) orbits of H-ions with gyro-radii 8, 10 and 12 cm and pitch-angle 63° (position of the IC resonance on the grid in figure 3) calculated back in time from the FILD scintillator plate.

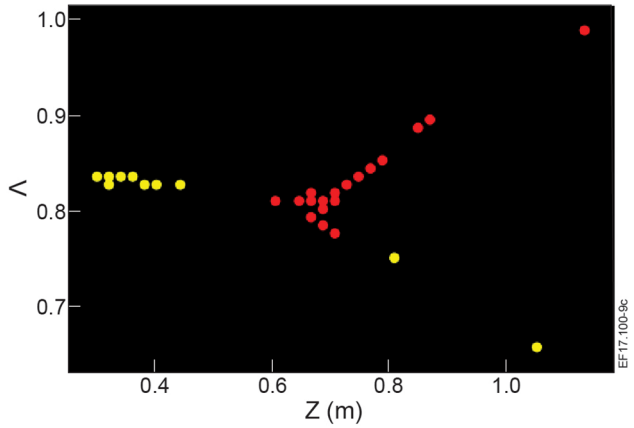

Figure 5. HAGIS calculation showing the region of constants-of-motion space (Λ, $Z_{R=R_{mag}}$, E) in which 3.0 MeV counter streaming protons undergo orbit topology changes as a result of their interaction with an ideal MHD $n = 1$ internal kink mode. The red points correspond to lost particles and the yellow points to trapped particles, which remain confined.

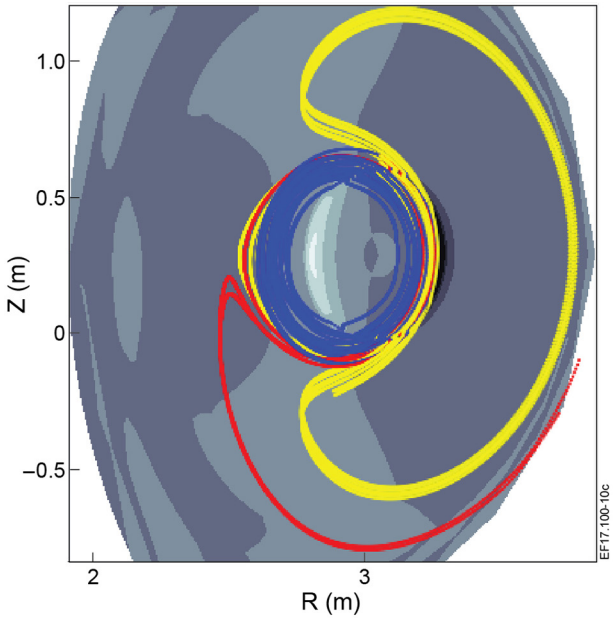

Figure 6. HAGIS calculation of perturbed proton orbits due to the assumed ideal internal kink mode. The orbits are chosen to correspond to those found near the mode-induced loss region of phase space given in figure 9, with the same colouring classification. The background shows the structure of the internal kink mode electrostatic potential.

shape as distributions before and after this period (although the total losses are higher); for tritons, the maximum of the losses is at $E_t \sim 1$ MeV, for protons at $E_p \sim 3$ MeV. However, the pitch-angle distribution of the prompt losses during the fishbone is slightly shifted relative to the FB-free distributions, from $\theta \sim 57°$ to ~55°. Assuming the losses are of the particles with trapped orbits, it is important to note that the major radius at the bounce reflection point for these particles and the pitch-angle value on the scintillator plate are related by $R(\theta) = R_{FILD}[1 - \cos^2(\theta)]$, where R_{FILD} is radial position of the scintillator. As can be seen from the differential loss footprint in figure 3(*b*), particles escaped during the FB period are mostly coming from the plasma region near 55° related to $R(55°) = 2.45$ m. A back-in-time FP orbit calculation starting from the FILD scintillator plate (figure 4(*a*)) shows that bounce points of these particles are close to the trapped/passing

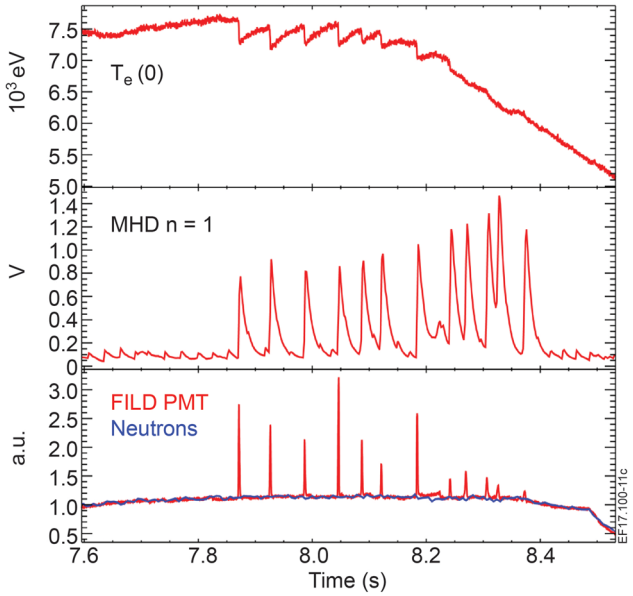

Figure 7. Fishbones lead to T_e drops in the plasma centre like sawteeth; neutron rate normalised to FILD losses during fishbone-free period is not affected by fishbones.

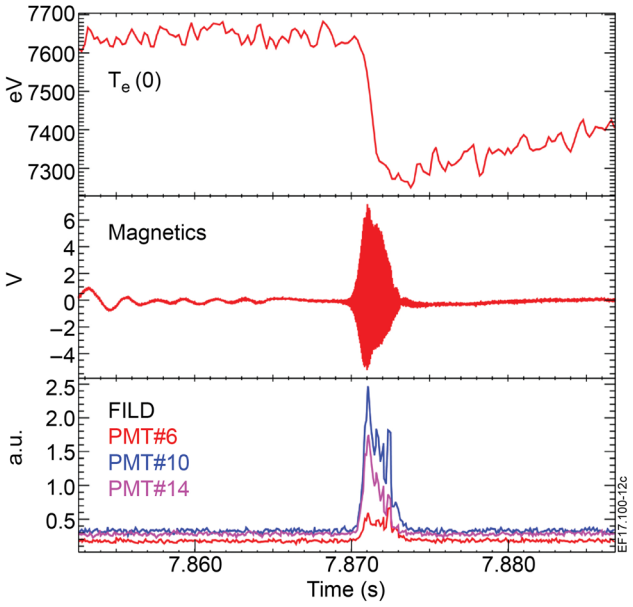

Figure 8. The first fishbone in the discharge (see figure 7): loss signals recorded with PMT #6, #10 and #14 (see figure 3(*b*)) drop at the same time as the fishbone amplitude.

boundary in the mid-plane at ~2.45 m. However, the orbits of H-ions accelerated by ICRH, calculated with pitch-angle $\theta \sim 63°$ are trapped and their turning points are on the IC resonance layer at $R \approx 2.97$ m (figure 4(*b*)). These calculations give us a proof that ions escaped from the plasma during the fishbone period are mostly fusion products.

An $n = 1$ ideal internal kink mode was found with the MISHKA-1 code [17] for a JET equilibrium reconstruction obtained with EFIT [18]. The HAGIS [19] code was used to compute the fusion product drift orbits assuming the EFIT equilibrium, and the drift orbit changes were computed

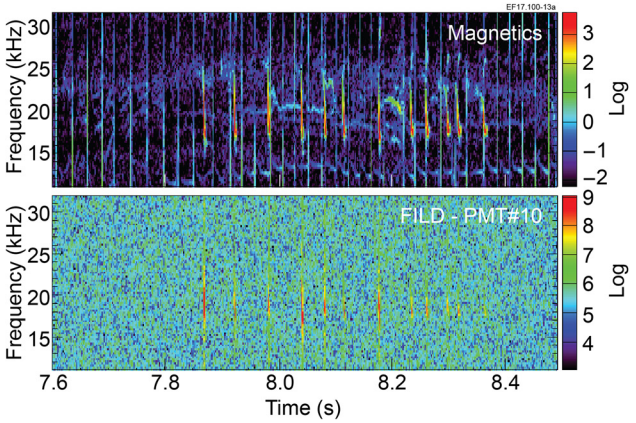

Figure 9. Fourier spectrograms of an in-vessel magnetic pickup coil with bursting fishbones and the FILD loss spectrogram that coherent to the fishbones in PMT #10 (see figure 3(*b*)).

assuming the MISHKA-1 solution (full details of these calculations will be the subject of a following publication). The largest losses are predicted for particles near the boundary between trapped and counter passing lost orbits. The results are shown in figure 5, where $Z_{R=R_{mag}}$ denotes the Z particle location in the upper midplane where it crosses $R = R_{mag}$. This is used in place of the canonical momentum P_φ. The three constants of motion used in the plots are Z (canonical momentum), Λ (magnetic moment) and energy E. The plots are at fixed E corresponding to the proton birth energy ignoring thermal spread. One can see that the lack of particles at the parameter $\Lambda = 1$ ($\Lambda \equiv \mu_m B(R_{mag})/E = B(R_{mag})[1 - \cos^2\theta]/B$) related to on-axis trapped orbits of H- and D-beam ions accelerated by ICRH is consistent with the footprint in figure 3(*b*). Figure 6 gives an illustration of the orbit types, where the greatest prompt fusion product losses are predicted to occur. The counter travelling fusion product orbits near the trapped/passing/lost triple-point cross the internal kink mode. So, the fishbone is producing a radial convection of these non-resonant fusion protons into loss regions.

It is important to emphasise that the D–D neutron rate was not affected by the $n = 1$ MHD activity related to the fishbones although $T_e(0)$ drops ~5%, which looks like sawteeth. However, this T_e drop is not so fast (~3–5 ms) as in a typical sawteeth (<1 ms). In figure 7 one can see that the normalised neutron rate follows the continuous losses related to prompt losses of fusion products and there are no evident drops of the rate during the loss spikes. So, despite the fishbones being driven by a resonant interaction with NBI ions, they do not appear to affect significantly the D-beam ion confinement, since no changes in the neutron rate are apparent. Also, it is likely some loss of H-minority ions that cannot be clearly identified with FILD is responsible for the relatively gradual drop in T_e.

The FP loss signals related to PMT #6, #10 and #14, whose fields of view areas are shown in figure 3(*b*) as white rectangles are roughly proportional to the FB oscillation amplitude (figure 8). However, a comparison with the MeV H-ion loss findings obtained by authors in [13], in particular

the quadratic increase with the FB amplitude, is not possible in this case; an accurate dependence of the FP loss versus the FB amplitude cannot be determined because most of the magnetic signals were saturated. One can see that the highest loss signals were recorded with PMT #10 and #14 and they are relevant to the prompt triton/protons losses. The measured losses are coherent to $m = 1/n = 1$ FB oscillations that can be clearly seen by comparing magnetic and FILD-PMT spectrograms shown in figure 9. This is yet further evidence of observation of fusion products loss induced by fishbones in the JET deuterium hybrid plasma.

The experimental observation and modelling of the non-resonant losses of fusion products caused by low-frequency fishbones are confirming the loss mechanism proposed in [12]. This effect could be important for fusion alpha-particles in burning plasma scenarios with fishbones e.g. hybrids.

Acknowledgments

This work has been carried out within the framework of the EUROfusion Consortium and has received funding from the Euratom research and training programme 2014–2018 under grant agreement No 633053 and from the RCUK Energy Programme (grant No EP/P012450/1). To obtain further information on the data and models underlying this letter please contact PublicationsManager@ukaea.uk. The views and opinions expressed herein do not necessarily reflect those of the European Commission.

References

[1] Fasoli A. *et al* 2007 *Nucl. Fusion* **47** S264–84
[2] Gormezano C. *et al* 2007 *Nucl. Fusion* **47** S285–336
[3] McGuire K. *et al* 1983 *Phys. Rev. Lett.* **50** 891
[4] Heidbrink W.W. *et al* 1986 *Phys. Rev. Lett.* **57** 835
[5] White R.B. *et al* 1986 1983 *Phys. Fluids* **26** 2958
[6] Coppi B. *et al* 1988 *Phys. Fluids* **31** 1630
[7] Borba D. *et al* 2000 *Nucl. Fusion* **40** 775
[8] Heidbrink W.W. and Sadler G.J. 1994 *Nucl. Fusion* **34** 535–615
[9] Heidbrink W.W., Chrien R.E. and Strachan J.D. 1983 *Nucl. Fusion* **23** 917–31
[10] Heidbrink W.W., Hay R. and Strachan J.D. 1984 *Phys. Rev. Lett.* **53** 1905–8
[11] Duong H.H. and Heidbrink W.W. 1993 *Nucl. Fusion* **33** 211–21
[12] Coppi B. *et al* 1988 *Fusion Technol.* **13** 447
[13] Perez von Thun C. *et al* 2010 *Nucl. Fusion* **50** 084009
Perez von Thun C. *et al* 2011 *Nucl. Fusion* **51** 053003
[14] Kiptily V.G. *et al* 2014 *Fusion Reactor Diagnostics: Proc. Int. Conf. (Monastero, Varenna, Italy, 9–13 September 2013)* vol 1612 (New York: AIP Publishing) pp 87–92
[15] Baeumel S. *et al* 2004 *Rev. Sci. Instrum.* **75** 3563
[16] Werner A., Weller A. and Darrow D.S. 2001 *Rev. Sci. Instrum.* **72** 780
[17] Mikhailovskii A.B. *et al* 1997 *Plasma Phys. Rep.* **23** 844 (in English)
[18] Lao L.L. *et al* 1985 *Nucl. Fusion* **25** 1611–22
[19] Pinches S.D. *et al* 1998 *Comput. Phys. Commun.* **111** 133
[20] Litaudon X. *et al* 2017 *Nucl. Fusion* **57** 102001